Pflügers Arch (1994) 428:364–371

Pflugers Archiv
European Journal of Physiology

Volume-activated Cl^- currents in different mammalian non-excitable cell types

Bernd Nilius, Jan Sehrer, Felix Viana, Christine De Greef, Luc Raeymaekers, Jan Eggermont, Guy Droogmans

KU Leuven, Laboratorium voor Fysiologie, Campus Gasthuisberg, B-3000 Leuven, Belgium

Received April 5, 1994/Received after revision and accepted June 1, 1994

Abstract. The existence and properties of volume-activated Cl^- currents were studied in 15 different cell types (endothelium: human umbilical vein, human aorta, bovine pulmonary artery; fibroblasts: Swiss 3T3, L, C3H $10T^1/_2$ and COS-1; epithelium: KB3, HeLa and A6; blood cells: RBL-2H3 and Jurkat; endothelioma cells derived from both subcutaneous and thymic hemangiomas; skin: IGR1 melanoma). Volume-activated Cl^- currents with common characteristics, i.e. small conductance, outward rectification, higher permeability for iodide than for chloride and sensitivity to block by 5-nitro-2-(3-phenylpropylamino)benzoic acid (NPPB) could be elicited in all cells. The block of this current by tamoxifen and dideoxyforskolin is different for the various cell types, as well as the time course and the amplitude of the responses induced by repetitive applications of hypotonicity. Volume-activated Cl^- channels with similar biophysical properties are therefore widespread among mammalian cells. This may reflect either a single Cl^- channel that is ubiquitously expressed or a family of functionally related Cl^- channels with cell specific expression patterns.

Key words: Endothelium – Fibroblasts – Tumour cells – Mast cells – Endothelioma cells – Volume regulation – Patch clamp – Chloride currents

Introduction

Cl^- channels activated by cell swelling have been observed in several cell types, such as chromaffin cells [4, 5], fibroblasts [23], Jurkat cells [12], epithelial cells [2, 11] and endothelium [15, 16]. The volume-activated channels from different cell types share some common properties, such as small conductance (less than 5 pS) and a higher permeability for iodide than chloride. Moreover, activation does not depend on intracellular Ca^{2+} but intracellular adenosine triphosphate (ATP) is required for a maintained channel activity. The protein kinase A (PKA) pathway is not involved in activation or modulation of this current. Large conductance (40–400 pS), volume-activated Cl^- channels have been reported as well [1, 13, 22], and recently a 19 pS channel has been described in osteoclasts [10]. Besides their obvious role in volume regulation, these currents are apparently involved in many other cell functions, e.g. mechanotransduction [18], regulation of intracellular pH via modulation of the Cl^-/HCO_3^-, $K^+/Na^+/2Cl^-$ transporters [20], modulation of Ca^{2+} sequestration [8] and volume control during mitosis [6].

The common properties may indicate either a single Cl^- channel that is widely expressed or a family of functionally related channels with cell-specific expression. Possible candidates are members of the ClC-x family (e.g. ClC-2 channels), I_{Cln} channels and P-glycoprotein (see [21] for a review). We were interested to see whether this volume-activated current is also present in cells other than those hitherto studied. The purpose of this screening was to find a cell line that lacks volume-activated currents. This would allow us to design molecular-biological strategies to evaluate further the appealing hypothesis that volume-activated Cl^- channels are associated with P-glycoprotein [7, 23].

In this study we have characterized volume-activated currents in 15 different cell types with respect to conductance, pattern of block, kinetics of activation and rectification. The current properties in most of the investigated cells are similar to those in endothelial cells. However, we describe here quantitative differences between different cell types in pharmacological features and in the responses to repetitive activation. Part of the results has been published in abstract form [17].

Materials and methods

Cell culture and cell types. Endothelial cells from human umbilical cord veins were obtained by a collagenase digestion procedure, as

Correspondence to: B. Nilius

described previously [15, 16]. Endothelial cells from human aorta and bovine pulmonary artery were from established cell lines. Other cell types used were: Jurkat (human acute T-cell leukemia), HeLa (human epitheloid carcinoma), rat RBL-2H3 cells (kindly provided by Dr. I. Pecht, Rehovot, Israel), Swiss 3T3 (mouse embryo fibroblasts, kindly provided by Dr. J. J. Cassiman, Leuven, Belgium), L cells (mouse connective tissue), A6 cells (toad kidney, courtesy of Dr. J. P. Johnson, Pittsburg, USA), COS-1 (monkey kidney), KB3 (human epitheloid cancer cells, kindly provided by Dr. B. Sarkadi, Budapest, Hungary), mouse endothelioma cell lines derived from subcutaneous (Endom-S) and thymic (Endom-T) haemangiomas (courtesy of Dr. M. Vidal, Milano, Italy), and mouse C3H $10T^1/_2$ fibroblasts. Cells were grown in appropriate tissue culture media supplemented with 10% human serum or fetal calf serum, 2 mmol/l L-glutamine, 100 kU/l penicillin and 100 mg/l streptomycin as required. The culture medium was exchanged every 48 h. Adherent cells were detached by exposure to 0.05% trypsin in a Ca^{2+}- and Mg^{2+}-free solution for approximately 180 s. Cells were reseeded on gelatin-coated coverslips at a density of 5,000–10,000 cells per coverslip. We kept the cells 2–4 days in culture prior to electrophysiological experiments.

Current measurements. Electrophysiological methods have been described in detail elsewhere [15]. Whole-cell membrane currents were measured using patches perforated with nystatin to avoid disturbance of the intracellular Ca^{2+}-buffering mechanisms [9]. Currents were monitored with a patch-clamp amplifier (EPC-7, List Electronic, Darmstadt, Germany or EPC-9, Heka Electronics, Lambrecht, Pfalz, Germany) and samples at 4-ms intervals (2048 points per record, filtered at 100 Hz). The voltage protocol consisted of a 1.2-s step to −80 mV, followed by a step of 0.4 s to −150 mV and a 5.2-s linear voltage ramp to +100 mV. This protocol was applied every 10 s from a holding potential of 0 mV. Such a protocol has the advantage that the time course of current activation and the voltage dependence of the current can be studied. The current/voltage (*I/V*) relationship of the volume-activated current and its reversal potential (V_{rev}) were obtained from difference currents measured during voltage ramps in isotonic and hypotonic solutions.

Solutions. The standard bath solution was a modified Krebs' solution of the following composition (in mmol/l): 132 NaCl, 1.5 $CaCl_2$, 5.9 KCl, 1.2 $MgCl_2$, 11.5 4-(2-hydroxyethyl)-1-piperasineethane sulphonic acid (HEPES)-NaOH, 10 glucose, titrated to pH 7.3 with NaOH. Osmolarity was 290 mosm/l. Hypotonicity was induced by diluting this solution to an osmolarity of 185 mosm/l with distilled water. Osmolarity of all the solutions was measured with a vapor pressure osmometer (Wescor 5500, Schlag Meßinstrumente, Gladbach, Germany). The standard pipette (internal) solution was made in deionized water (Milli-Q, Millipore) and contained (in mmol/l): 100 K-aspartate, 40 KCl, 4 Na_2-ATP 10 HEPES, 0.1 ethylene bis(oxonitrilo)tetraacetic acid (EGTA) buffered at pH 7.2 with KOH, 290 mosm/l. For permeation measurements, we used the same solutions as Diaz et al. [2], i.e., an isotonic bath solution containing (in mmol/l): 105 NaCl, 0.5 $MgCl_2$, 10 HEPES and 70 D-mannitol, adjusted to pH 7.3 with NaOH. This solution was made hypotonic by omitting the D-mannitol. The pipette solution contained (in mmol/l): 105 KCl, 1.2 $MgCl_2$, 10 HEPES, 70 D-mannitol, 4 Na_2ATP, 1 EGTA (KOH). For the anion substitution experiments, NaCl in the hypotonic solution was replaced by NaI or Na gluconate. For the experiments with gluconate we corrected the Ca^{2+}-chelating effect of this anion to avoid changes in extracellular $[Ca^{2+}]$ ($[Ca^{2+}]_e$). Experiments were performed at room temperature (20–22° C).

The following substances were used to modulate volume-activated currents: 5-nitro-2-(3-phenylpropylamino)-benzoic acid (NPPB, kindly provided by Dr. Lang, Hoechst, Frankfurt, Germany) and 1,9-dideoxyforskolin (DDFSK, Sigma).

Statistics. Pooled data are given by mean ± SEM. For significance, Student's *t*-test was used (level of significance, $P < 0.05$). Fitting routines were used from the software package Origin (MicroCal Software, Northampton, USA).

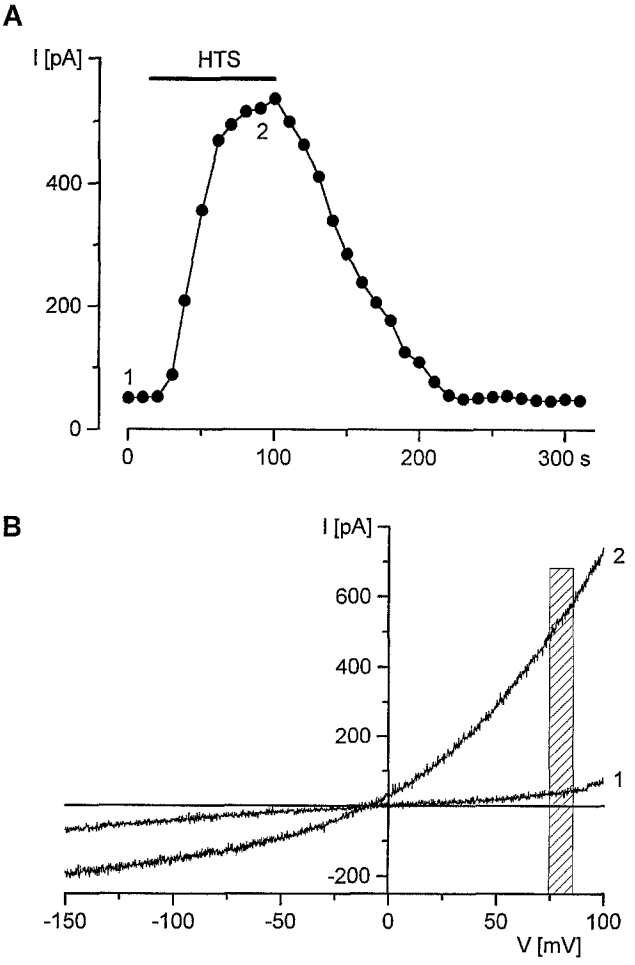

Fig. 1A, B. Volume-activated Cl^- current in endothelial cells from human umbilical vein. **A** Time course of the HTS-activated current at +80 mV. Data points were calculated as the average current in a voltage window from +75 to +85 mV (indicated by the *shaded area* in **B**) during voltage ramps, which were repeated every 10 s. The *horizontal bar* indicates the period of hypotonicity. **B** Current-voltage (*I/V*) relationships derived from voltage ramps applied at the points labeled *1* and *2* in panel **A** (HTS hypotonic solutions)

Results

Volume-activated Cl^--currents in various cell types

Figure 1 shows the time course and voltage dependence of volume-sensitive Cl^- currents in umbilical vein endothelial cells activated by hypotonic solutions (HTS). Typical *I/V* curves before (1) and during (2) maximal activation of the current are shown in Fig. 1B. The V_{rev} of the volume-activated current, obtained from the difference current of these two traces, was around −8 mV, which is close to the Cl^- equilibrium potential of −18 mV. Time-dependent changes of the current were assessed from the averaged currents in the voltage window 75–85 mV (indicated by the shaded rectangle) during consecutive traces and represented in Fig. 1A as a function of time. The maximal increase in current amplitude during HTS compared with the background current in isotonic solutions was used to quantify the expression of volume-activated currents in various cell types. For

Table 1. Volume-activated Cl^- currents in various cell types. Experimental values represent current densities expressed per unit cell capacitance at +80 mV. Data are given as mean ± SEM (*n* number of cells tested, I_{Cl} current density)

	Cell type	Species	I_{Cl} (pA/pF)	*n*
Endothelium	umbilical vein (HUVEC)	human	21.3 ± 1.3	48
	aorta (EN-aorta)	human	28.2 ± 7.7	3
	pulmonary artery (CPAE)	bovine	22.1 ± 4.4	4
Fibroblast	Swiss 3T3	mouse	21.2 ± 1.6	15
	C3H $10T^1/_2$	mouse	13.9 ± 1.8	4
Connective tissue	L	mouse	10.2 ± 1.9	4
Fibroblast-like	COS-1	monkey	28.1 ± 2.2	5
Epithelium	HeLa	human	31.0 ± 5.0	11
	KB3, lung cancer	human	42.2 ± 2.5	30
	A6	toad	35.0 ± 3.2	8
Mast cells	RBL-2H3	rat	7.5 ± 1.0	23
T-lymphocytes	Jurkat	human	52.1 ± 7.2	22
Skin	melanoma, IGR1	human	18.6 ± 3.8	3
Hemangiomas	endothelioma-S (Endom-S)	mouse	16.0 ± 4.1	5
	endothelioma-T (Endom-T)	mouse	19.4 ± 7.6	10

comparative purposes, these values are expressed per unit cell capacitance. The data, summarised in Table 1, show that volume-activated currents can be evoked in all these cells. Current densities range from about 7 pA/pF in RBL-2H3 cells to values around 50 pA/pF in Jurkat cells.

However, these currents show some obvious differences between different cell types. Figure 2–4 show representative currents measured from C3H $10T^1/_2$ (mouse fibroblast), RBL-2H3 (rat mast cells) and 3T3 (mouse fibroblast). Challenge of the C3H $10T^1/_2$ cells with HTS induced a rapid increase in current at −80 and +80 mV, which could be activated repetitively and was completely blocked with 50 µmol/l NPPB (Fig. 2A). This repetitive activation is also a typical feature of the volume-activated current in endothelial cells from human umbilical vein [15]. Fig. 2B shows *I/V* relationships reconstructed from linear voltage ramps. The volume-activated current reversed at −15 mV which is close to the expected reversal potential of Cl^-.

In mast cells (Fig. 3A) there is virtually no activation of current at negative voltages, whereas the rate of current activation and of recovery at +80 mV is very slow. In addiiton, the response to a second HTS challenge is much smaller than that observed during the first exposure to HTS. Challenge of the cells with HTS in the presence of 50 µmol/l NPPB did not induce any current (first HTS stimulation in Fig. 3A; five cells). Because it turned out to be difficult to activate the current in RBL cells repetitively, we applied NPPB before the control stimulation with HTS. Figure 3B shows *I/V* curves for these cells before (1), during (2) and after (3) exposure to hypotonic solutions. The volume-activated current at negative potentials is masked by a large inwards-rectifying current component at negative potentials, that is characteristic for these cells. Nevertheless, current activation by HTS is less pronounced at negative potentials, resulting in a pronounced outwards rectification of the volume-activated current. The increase of the current beyond the holding current at any potential is smaller in RBL cells than in C3H $10T^1/_2$ cells (compare Figs. 2B and 3B). The pronounced differences in the time course of activation of the HTS currents in RBL cells and another cell line (3T3 fibroblasts) are obvious from Fig. 4A which shows superimposed normalized current traces for each cell type. Activation of the current in RBL cells is also much slower than in C3H $10T^1/_2$ cells and human umbilical vein endothelial cells. The time for half-maximal activation of the current at +80 mV was 95 ± 17 s in RBL cells ($n = 3$), compared with 29 ± 9 s ($n = 6$) for human umbilical vein endothelium and 32 ± 8 s ($n = 3$) for C3H $10T^1/_2$ cells. Slower activation of the volume-activated current was also observed in Jurkat cells. Figure 4B shows normalized *I/V* relations for the HTS-induced currents in RBL-2H3 and 3T3 cells. It is clear that the degree of rectification of the volume-activated Cl^- current is similar in both cell types, in spite of the obvious differences in their rate of activation.

Conductance properties

Another feature of volume-activated Cl^- channels is a small conductance in the range of less than 5 pS [11, 12]. We have determined a single channel conductance in the same range in endothelial cells of human umbilical vein based on an analysis of the current fluctuations [15]. We have used this same technique to estimate the single channel conductance of volume-activated channels in several cell types. Figure 5 shows an example obtained from HeLa cells. Full activation of the current occurs in about 100 s. The current variance signals from traces lasting 1 s can therefore be regarded as stationary. Average current and current variance calculated from consecutive traces are shown as a function of time in Fig. 5A. It is obvious that the increase in average current is accompanied by an increase in current variance. Plots of the current variance (σ^2) as a function of the average current I can be described by

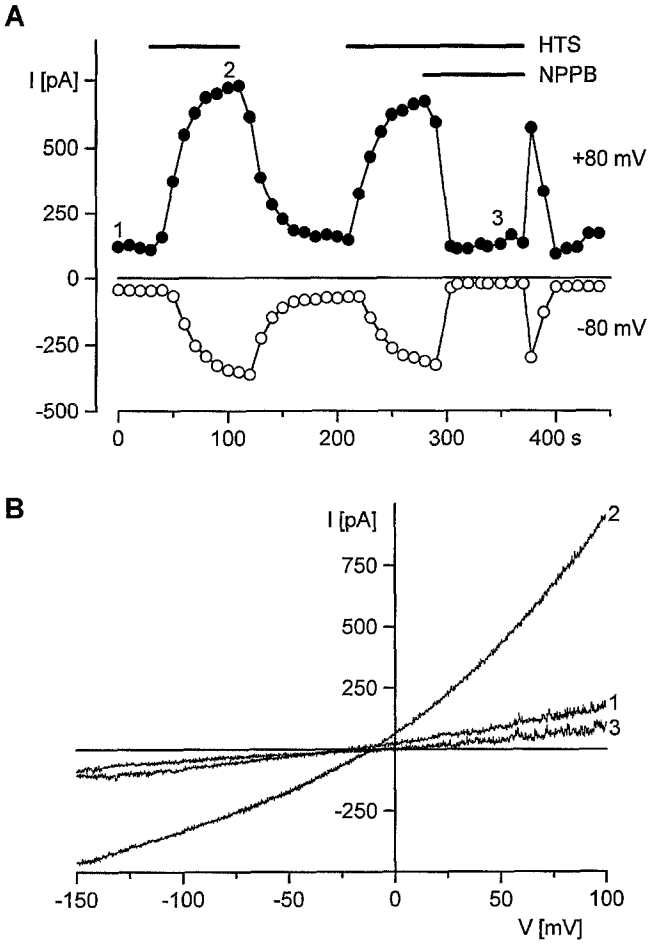

Fig. 2A, B. Volume-activated current in C3H $10T^1/_2$ mouse fibroblasts. **A** Repetitive activations, indicated by the *horizontal bars*, of the HTS-induced current at −80 and +80 mV. Points were calculated from currents in a small voltage window around each potential. **B** Representative *I/V* curves obtained at the times marked by *numbers* in **A** [**NPPB** 5-nitro-2-(3-phenylpropylamino)benzoic acid]

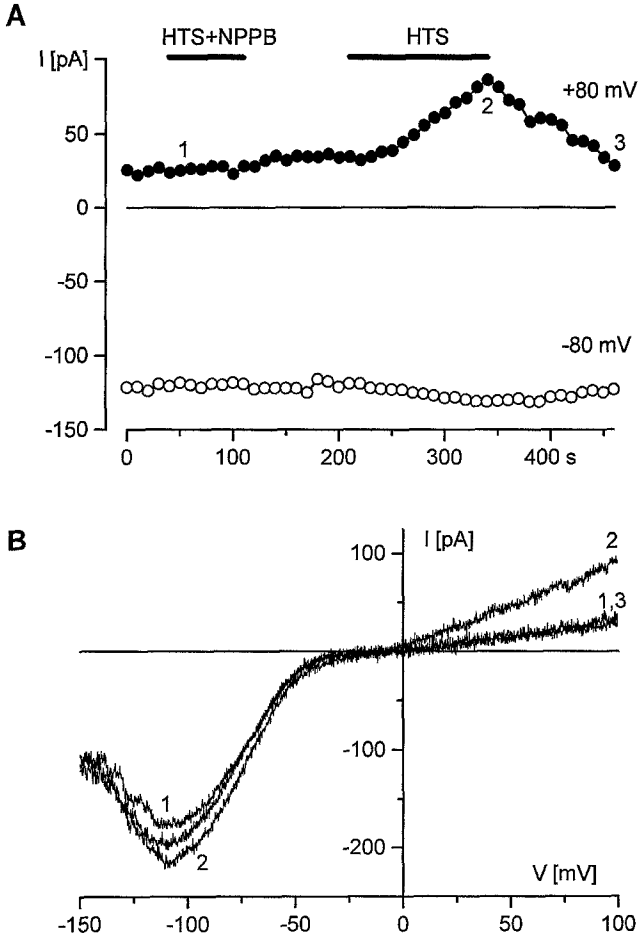

Fig. 3A, B. Volume-activated current in RBL-2H3 rat mast cells. Time course of HTS-activated current (**A**) and *I/V* curves (**B**) obtained by a protocol similar to that employed in Fig. 2. NPPB was applied before the control stimulation with HTS, because of the rapid run-down of the HTS-induced current in these cells during repeated stimulations

$$\sigma^2 = i \cdot I - I^2/N \quad (1)$$

were i is the single channel current and N the number of channels. Figure 5B shows such a plot together with the fitted curve. The single channel conductance, calculated from i derived from this fit and the driving force of Cl^-, was 0.9 pS. The results of this fluctuation analysis for the various cell types are summarized in Table 2. In most experiments, we could only obtain data points from the ascending limb of the parabola, suggesting that the probability of the channels being open is small. It is still possible to obtain a reliable estimate of i from this ascending limb, but not of N. The latter values are therefore not included in Table 2.

Permeation properties

A characteristic property of volume-activated Cl^- channels in most cells is their anion permeability. Volume-activated Cl^- channels in chromaffin cells [3], HeLa cells [2], Jurkat cells [12] and umbilical vein endothelial cells [16] are more permeable for iodide than for chloride. We have now extended these measurements to various other cell types. Figure 6 shows an example for 3T3 fibroblasts and RBL cells. The volume-activated current, as determined by subtraction of stationary *I/V* relationships before and during perfusion of the cells with HTS, were measured under various anionic conditions and their V_{rev} determined. Under conditions with symmetrical $[Cl^-]$ V_{rev} was close to 0 mV. Substitution of extracellular Cl^- with iodide or gluconate shifted V_{rev} to more negative or more positive potentials respectively (Fig. 6A, B). From V_{rev} under these asymmetric anion conditions we calculated the permeability of these anions relative to that of Cl^- by means of the Hodkin-Huxley-Katz equation

$$\frac{P_x^-}{P_{Cl^-}} = \frac{[Cl^-]_i \cdot \exp(-F \cdot V_{rev}/RT) - [Cl^-]_e}{[X^-]_e} \quad (2)$$

where R, T, F have their usual meaning, P_x^- and P_{Cl^-} represent the permeabilities of the test anion X^- and Cl^- and the subscripts i and e indicate intra- and extracellular

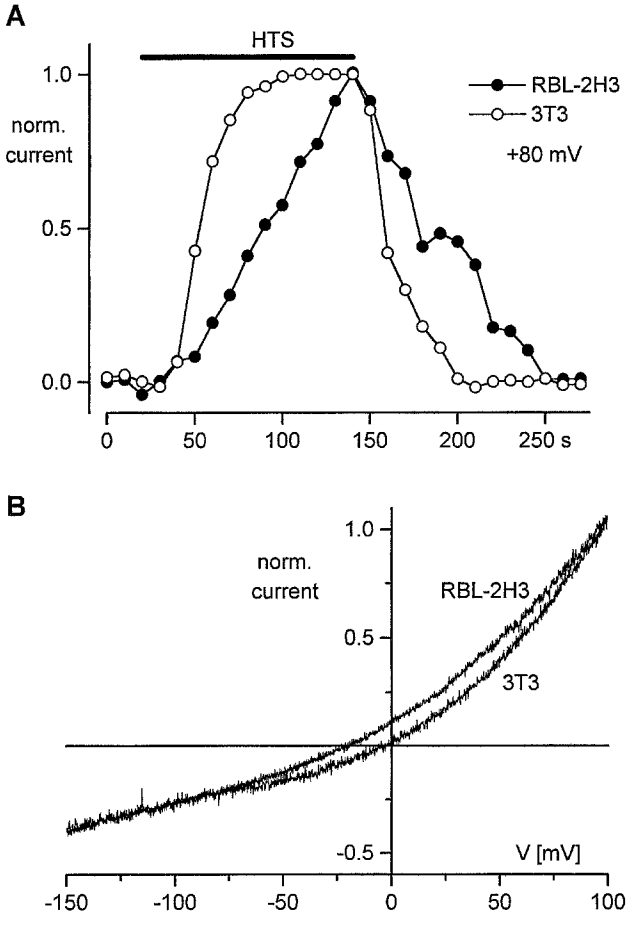

Fig. 4A, B. Comparison of HTS-activated currents in RBL-2H3-mast cells and 3T3 mouse fibroblasts. **A** Time course of normalized HTS-activated currents at +80 mV in RBL (*filled circles*) and 3T3 (*open circles*) cells. Data points were calculated as the average current in a voltage window from +75 to +85 mV and normalized to the maximum current observed in each cell during hypotonic challenge. **B** *I/V* curves of the HTS-induced current normalized to the maximum value at +100 mV in both cell types

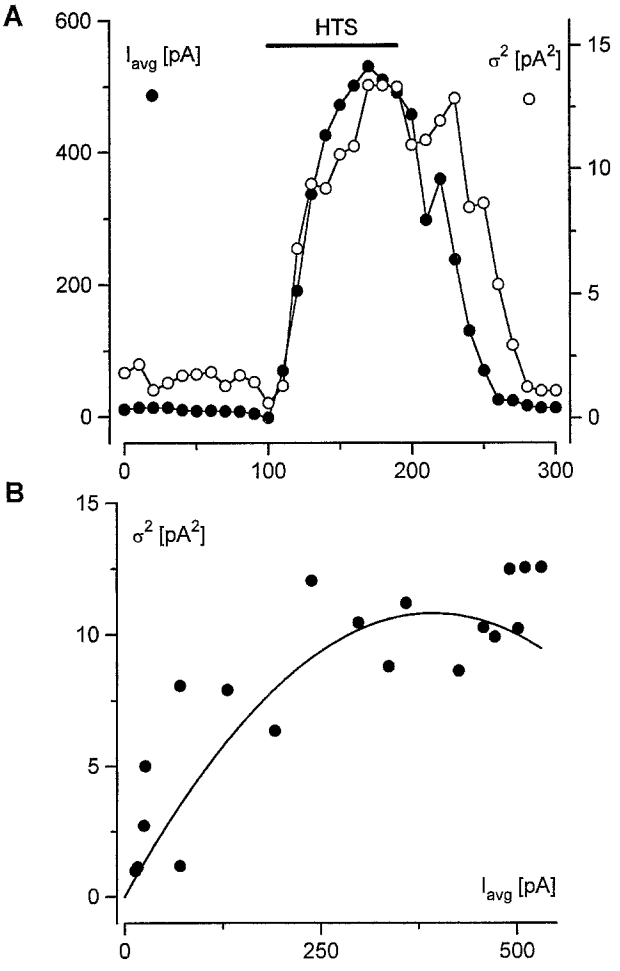

Fig. 5A, B. Fluctuation analysis of the HTS-activated Cl^- current in a HeLa cell. **A** Time course of average current and current variance during application of HTS. Data were calculated from consecutive current traces during the initial voltage step to −80 mV in the voltage protocol. **B** Plot of current variance vs. average current during HTS and recovery from HTS. The *solid line* represents the fit of the data points to equation (1) in text (I_{avg} average current, absolute values, σ^2 current variance)

respectively. The results from this analysis for 3T3 and RBL-2H3 cells are shown as insets in Fig. 6A and B. In all cells tested we found a higher permeability for iodide than for chloride. These results, together with some data from the literature, are summarized in Table 2.

Repetitive activation of the HTS current

The volume-sensitive current has been reported to be capable of being activated only once in chromaffin cells [3], whereas it can be activated without significant "run-down" up to 30 times or more in human endothelial cells [15, 19]. A similar feature was observed in KB3 cells (Fig. 7A), 3T3 and C3H $10T^1/_2$ fibroblasts. Volume-activated Cl^- currents in HeLa cells (Fig. 7B) and endothelioma cells seem to run down much faster than in endothelial cells. A fast run-down occurred in RBL-2H3 cells and sometimes the current was completely absent during a second HTS challenge (Fig. 7C). We have shown previously that run-down can be induced in endothelial cells by depleting them of intracellular ATP [19]. It is therefore possible that this run-down is related to the metabolic state of the cell, rather than being an intrinsic property of the channel.

Pharmacological properties

Volume-activated Cl^- currents could be completely and reversibly blocked by 100 μmol/l NPPB in all cells tested (see Fig. 2A for C3H $10T^1/_2$ cells, Fig. 3 for RBL cells, Fig. 7B for HeLa cells, Fig. 7A for KB3 cells). Such a uniform response was however not observed with other blockers such as DDFSK and tamoxifen, substances which block the multidrug resistance (P-glycoprotein) transporter and the presumed P-glycoprotein-associated Cl^- channels [14]. HeLa cells and endothelial cells have been shown to be sensitive to blockers of the

Table 2. Single channel conductance and permeation properties of volume-activated Cl^- channels. Data are means ± SEM (γ single channel conductance, P permeability, n number of cells, – not determined)

Cell type	γ (pS)	n	P_I/P_{Cl}	n	P_{gluc}/P_{Cl}	n
HUVEC	1.1 ± 0.12[1]	34	1.63 ± 0.30[1]	10	0.20 ± 0.07[1]	10
EN-Aorta	1.5		–		–	
COS-1	0.4		–		–	
HeLa	2.8 ± 1.2	4	–		–	
KB3	3.2 ± 1.6	4	1.26 ± 0.01	9	0.18 ± 0.009	11
3T3	1.4 ± 0.4	5	1.68 ± 0.19	10	0.30 ± 0.06	7
RBL-2H3	5.8 ± 2.1	4	1.2 ± 0.12	10	0.22 ± 0.08	10
Jurkat	2.4 ± 0.8[2]	3	1.35 ± 0.1[2]	4	0.10 ± 0.06[2]	13
C3H $10T^1/_2$	0.2		–		–	
Endom-S	–		2.18 ± 0.24	10	0.1 ± 0.04	10
Endom-T	–		2.22 ± 0.17	6	0.03 ± 0.02	4
L	1.9	2	1.21 ± 0.05	6	0.24 ± 0.04	5

[1] From [15]
[2] From [12]

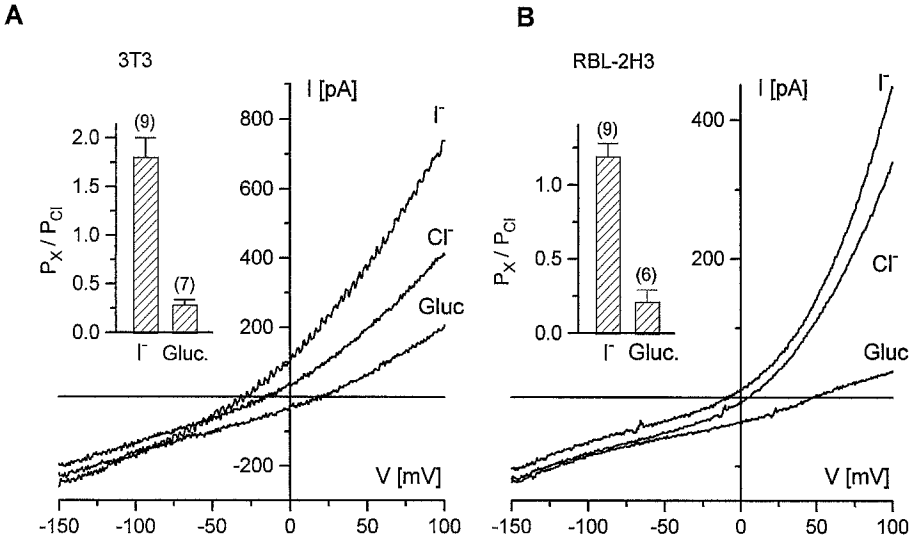

Fig. 6. Effect of anion substitution on current-voltage curves of HTS induced currents in 3T3 (**A**) and RBL-2H3 (**B**) cells. The permeability ratios of I^- and gluconate relative to that of Cl^- were calculated from the reversal potentials of the *I/V* curves, using equation (2) in text. The *inset* shows the results of these calculations for these two cell types (P_x permeability of cell membrane for x)

P-glycoprotein transporters, such as DDFSK and verapamil [2, 15]. Figure 8 shows another example of blockade of the volume-activated current by 50 µmol/l DDFSK in 3T3 fibroblast cells. Other cells, such as RBL cells, were however not sensitive to DDFSK. Chromaffin cells are also insensitive to DDFSK (E. Neher, personal communication). These different sensitivities to DDFSK may be important, because block by DDFSK has been used as an argument that P-glycoprotein might be associated with activation of the Cl^- channel.

The anti-oestrogen tamoxifen has been reported to be a high affinity blocker of the P-glycoprotein associated Cl^- channel [14]. We have previously shown that it induces a slow block and unblock of volume-activated Cl^- currents in endothelial cells [16]. Because of its supposed high affinity and P-glycoprotein specificity we tested this blocker in other cell types. Figure 8B shows the effect of 10 µmol/l tamoxifen on the volume-activated Cl^- current in RBL cells. Tamoxifen inhibited the HTS-activated current, however much more slowly than NPPB or DDFSK. Also the reversal of the block proceeds over a time course of several seconds. The blocking effects of these various compounds, expressed as a percentage reduction of the volume-activated current, are summarized in Table 3.

Discussion

The Cl^- channels are of special importance for cell functions such as volume regulation, mechanosensitivity and modulation of membrane potential. Many cell types seem to express volume-activated Cl^- channels, the activation of which often elicits large currents. We have made a comparative study of these channels in various tissues and cell types in order to make a meaningful classification of these channels and to design a molecular-biological approach to identify the encoding genes. The response to a challenge with HTS was investigated in 15 different cell types, of which showed volume-activated currents.

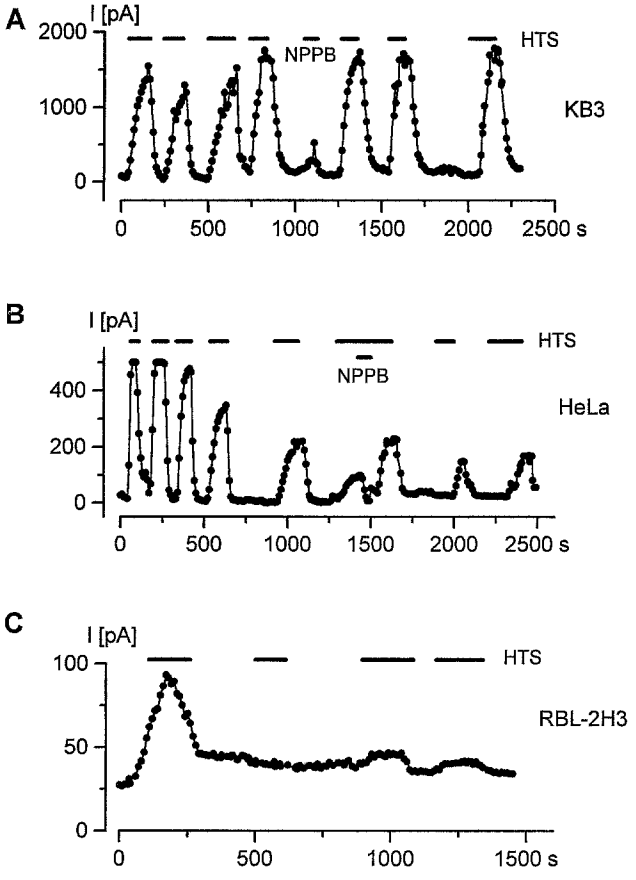

Fig. 7A–C. Pattern of repetitive current activation by HTS in various cell types (shown at the *right*)

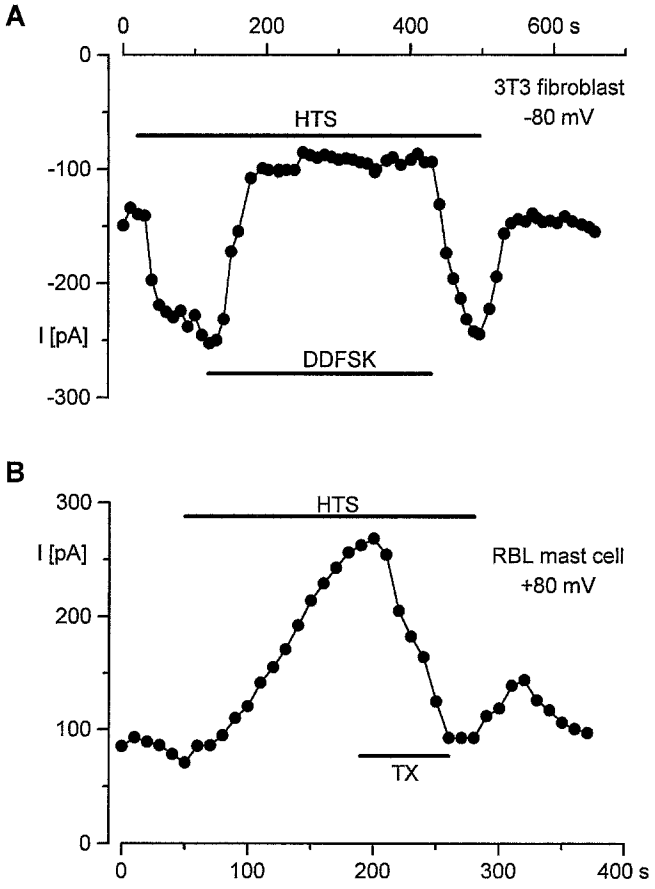

Fig. 8A, B. Pharmacological properties of HTS-induced currents. **A** Sensitivity of 3T3 fibroblasts to 50 µmol/l DDFSK, a blocker of P-glycoprotein-mdiated transport. **B** Block by 10 µmol/l tamoxifen of the HTS-induced current in RBL cells. Average currents at +80 mV were calculated during successive voltage protocols (*DDFSK* dideoxyforskolin, *TX* tamoxifen)

These currents share a number of common characteristics, such as small conductance of less than 5 pS, outward rectification, higher permeability for iodide than for chloride and a block by NPPB. Similar features have previously been observed in other cell types such as chromaffin cells [4]. T-lymphocytes [12], epithelial cells [10] and endothelial cells [15]. The widespread occurrence of volume-activated Cl^- channels with nearly identical biophysical properties points either to a single, ubiquitously expressed Cl^- channels or to a family of functionally similar Cl^- channels. Our present data do not allow discrimination between these two possibilities.

However, there also exist some obvious differences between the currents measured in the various cell types. The kinetics of activation in RBL cells are much slower than in the other cells, for which endothelial cells might serve as a paradigm. In addition, the responses during repetitive stimulations run down rapidly in these cells. These properties are similar to those of chromaffin cells, in which the volume-activated current can be activated only once. This rapid run down may, however, be related to the metabolic state of the cell, rather than being an intrinsic channel property, because we were able to induce this run-down in endothelial cells by depleting them of intracellular ATP.

Another striking difference is the different sensitivity of the volume-activated current in the various cell types for compounds, such as the anti-oestrogen tamoxifen and DDSFK, which are supposed to block P-glycoprotein-associated Cl^- channels [2, 14]. Endothelial cells were sensitive to both DDFSK and tamoxifen (in the micromolar range, [15, 16]), whereas L and RBL cells were much less affected by tamoxifen in concentrations that blocked Cl^- channels in endothelial cells, 3T3 fibroblasts and lung epithelial cancer cells (see also [14]). DDFSK was much less effective in L-fibroblasts, KB3 cancer cells, RBL cells, endothelioma cells and Jurkat cells (see also [12]). The different sensitivities to DDFSK and tamoxifen raises the question of how these Cl^- channels are related to MDR1 P-glycoprotein. DDFSK and tamoxifen have indeed been proposed as specific inhibitors of P-glycoprotein associated Cl^- channels [14]. If so, then some of the currents that we have observed would belong to this class of P-glycoprotein-associated Cl^- channels, whereas the others would belong to a different class. However, because of their common biophysical profile we prefer to categorize these volume-activated currents as a single class of functionally related channels, irrespective of their sensitivities to DDFSK and tamoxifen. It is therefore question-

Table 3. Sensitivity to block by NPPB, dideoxyforskolin and tamoxifen. Effects are expressed as percentage inhibition of the current induced by cell exposure to hypotonic solutions, i.e., 100. $(I_{cont}-I_{test})/I_{cont}$, where I_{cont} and I_{test} are the current values before and during application of the test compound. Data are means ± SEM (*NPPB* 5-nitro-2-(3-phenylpropylamino)benzoic acid, *DDFSK* dideoxyforskolin, *n* number of cells, – not determined)

Cell Type	NPPB 50 μM	*n*	DDFSK 50 μM	*n*	Tamoxifen 10 μM	*n*
HUVEC	71 ± 7[2]	4	100[1]	9	88 ± 11[2]	5
C3H 10T½	100[2]	1	–		–	
3T3	100	3	block[3]		100 and block[3]	
L	100	6	no effect		11 ± 6	4
COS-1	100	3	–		–	
KB3	95 ± 2	26	38 ± 12	10	47 ± 8	5
HeLa	91 ± 6	22	31 ± 4	18	65 ± 7	3
Endom-S	100	2	17 ± 3.5	3	no response	1
Endom-T	100	3	11 ± 8	3	–	
Jurkat	100	2	no effect[4]		–	
RBL-2H3	80 ± 9	3	no effect		33 ± 11	5

[1] 100 μM, from [15]
[2] From [13]
[3] From [14]
[4] From [12]

able whether these compounds can be used to discriminate between volume-activated Cl^- channels.

In conclusion, our data support the idea that expression of volume-activated Cl^- channels is a widespread, if not ubiquitous, property of mammalian cells. Taking into account the striking biophysical similarities of these currents in the various cell types, they may belong to a functionally homogeneous family of channels which seems to be expressed in most non-excitable cells.

Acknowledgements. B. N. was supported by the Max-Planck-Gesellschaft, Germany. J. E. is a post-doctoral Researcher of the Belgian National Fund for Scientific Research (NFWO, Belgium). J. S. was supported by a grant from the Studienstiftung des Deutschen Volkes. F. V. was supported by a fellowship from the CICYT of the Spanish Government.

References

1. Baer CE (1994) Drugs transported by P-glycoprotein inhibit a 40 pS outwardly rectifying chloride channel. Biochem Biophys Res Commun 200: 513–521
2. Diaz M, Valverde MA, Higgins CF, Rucareanu C, Sepulveda FV (1993) Volume-activated chloride channels in HeLa cells are blocked by verapmil and dideoxyforskolin. Pflügers Arch 422: 347–353
3. Doroshenko P (1991) Second messengers mediating activation of chloride current by intracellular GTPγS in bovine chromaffin cells. J Physiol (Lond) 436: 725–738
4. Doroshenko P, Neher E (1992) Volume-sensitive conductance in bovine chromaffin cell membrane. J Physiol (Lond) 449: 197–218
5. Doroshenko P, Penner R, Neher E (1991) A novel chloride conductance in the membrane of bovine chromaffin cells activated by intracellular GTPγS. J Physiol (Lond) 436: 711–724
6. Dubois J-M (1991) Role of potassium channels in mitogenesis. Prog Biophys Mol Biol 59: 1–21
7. Gill DR, Hyde SC, Higgins CF, Valverde MA, Minteng GM, Sepulveda FV (1992) Separation of drug transport and chloride channel functions of human multidrug resistance P-glycoprotein. Cell 71: 23–32
8. Hofer AM, Machen TE (1993) Technique for in situ measurement of calcium in intracellular inositol 1,4,5 triphosphate-sensitive stores using the fluorescent indicator mag-fura-2. Proc Nat Acad Sci USA 90: 2598–2602
9. Horn R, Marty A (1988) Muscarinic activation of ionic currents measured by a new whole-cell recording method. J Gen Physiol 92: 145–159
10. Kelly MEM, Dixon SJ, Sims SM (1994) Outwardly rectifying chloride current in rabbit osteoclasts is activated by hyposmotic stimulation. J Physiol (Lond) 475: 377–389
11. Kunzelmann K, Kubitz R, Grolik M, Wart R, Greger R (1992) Small-conductance Cl^- channels in HT_{29} cells: activation by Ca^{2+}, hypotonic cell swelling and 8-Br-cGMP. Pflügers Arch 421: 238–246
12. Lewis RS, Ross PE, Cahalan MD (1993) Chloride channels activated by osmotic stress in T lymphocytes. J Gen Physiol 101: 801–826
13. Marunaka Y, Eaton DC (1990) Chloride channels in the apical membrane of a distal nephron A6 cell line. Am J Physiol 258: C352–C368
14. Mintenig GM, Valverde MA, Sepulveda FV, Gill DR, Hyde SC, Higgins CF (1994) Specific inhibitors distinguish the chloride channel and drug transporter functions associated with the human multidrug resistance P-glycoprotein. Receptors Channels 1: 305–313
15. Nilius B, Oike M, Zahradnik I, Droogmans G (1994) Activation of Cl^- channels by hypotonic stress in human endothelial cells. J Gen Physiol 103: 787–805
16. Nilius B, Sehrer J, Droogmans G (1994) Permeation properties and modulation of volume-activated Cl^-currents in human endothelial cells. Br J Pharmacol (in press)
17. Nilius B, Sehrer J, Viana F, Raeymaekers L, De Greef C, Droogmans G (1994) Properties of volume-activated chloride channels in various cell types. Pflügers Arch [Suppl] 427: R59
18. Oike M, Droogmans G, Nilius B (1994) Mechanosensitivity of endothelial cells is mediated by arachidonic acid. Proc Nat Acad Sci USA 91: 2940–2944
19. Oike M, Droogmans G, Nilius B (1994) The volume-activated chloride current in human endothelial cells depends on intracellular ATP. Pflügers Arch 427: 184–186
20. Parker JC (1993) In defense of cell volume? Am J Physiol 265: C1191–C1200
21. Paulmichl M, Gschwentner M, Wöll E, Schmarda A, Ritter M, Kanin G, Ellemuter H, Waitz W, Deetjen P (1993) Insight into structure-function relation of chloride channels. Cell Physiol Biochem 3: 374–387
22. Schwiebert EM, Mills JW, Stanton BA (1994) Actin-based cytoskelton regulates a chloride channel and volume in a renal cortical collecting duct cell line. J Biol Chem 269: 7081–7089
23. Valverde MA, Diaz M, Sepulveda M, Gill DG, Hyde SC, Higgins CF (1992) Volume regulated chloride channels are associated with the human multidrug-resistance P-glycoprotein. Nature 355: 830–833